Two-photon laser writing of micro-optics

Ching-Ting Tsai, Yi-Shiou Duh

Mentors: Vijay Narasimhan, J Provine, Swaroop Kommera

Abstract

Two-photon polymerization (TPP) is a technique to engineer high fidelity 3D structure with resolution down to 100 nm. Based on the interaction of highly localized femtosecond laser radiation with photosensitive material, TPP has become a cost-effective, high resolution, and good 3-D micro/nanoprinting strategy. Using the Nanoscribe Photonics GT system, we launched a project focusing on miniaturizing micro-optics printing. The ultimate goal of this study is to produce a cost-effective endoscope engineering for neuroscience applications. As a benchmark of engineering endoscope, this project showcases the microlens fabrication and identify chanllenges and propose corresponding solutions. We demonstrate a the process flow from design, manufacturing, characterizations, post-processing, and functionalities. This project aims to establish a useful and robust workflow for micro-optics fabrication to benefit photonics and micro/nano-fabrication community.

Contents

1 Introduction

Lens systems are ubiquitous in everyday life and have considerably developed in terms of complexity. Lens miniaturization is a growing field, and it drives revolutions in many research areas. For example, in electronics, the printed micro-optics could integrate with the CMOS chip to increase its detection sensitivity[7]. In neuroscience, people have striven to minimize endoscope footprint, and miniaturizing optical components is a critical topic[6, 1, 5]. Driven by an idea to produce a better biological probe for neuroscience, we launched a project to engineer endoscopes with small footprints using two-photon polymerization.

This project focuses on printing micro-optics as a benchmark of engineering endoscopes because this component plays an essential role in endoscope functionalities. Traditional lens fabrication involves drop-casting the polymer into the prefabricated structures or thermal reflow of polymers to form the curved microlenses[8]. However, the etching and the reflow strategies cannot control the curvatures precisely. Two-photon polymerization is ideal because it is cost-effective and has free-form design capabilities. Researchers have demonstrated printed single micro-lenses on CMOS or optical fiber to demonstrate some imaging applications[2, 3, 7]. However, this project aims to leverage the power of microlenses to a system level. By including multiple optical components within one design, we can stack multiple arbitrarily shaped lenses and demonstrate a fully functional relay optics system. As a result, we hope to engineer an optical imaging system with a large field of view and the least aberrations for a successful endoscopic application.

The printing process can benefit the Stanford nanofabrication community or any current Nanoscribe users. This project demonstrates the process flow from design, manufacturing, characterization, post-processing, and functionalities. We develop these process standards of procedures and include them in this document.

Please also visit our website (https://tingtsai.github.io/PrintableOptics/) to get our latest updates for this project.

2 Methods

2.1 Process flow and optimization metrics

The process of microlens fabrication includes three processes - File generation, 3-D printing, and Lens Optimization. Each step has its critical factors, and we design corresponding metrics and characterization strategies to evaluate those factors (Figure 1).
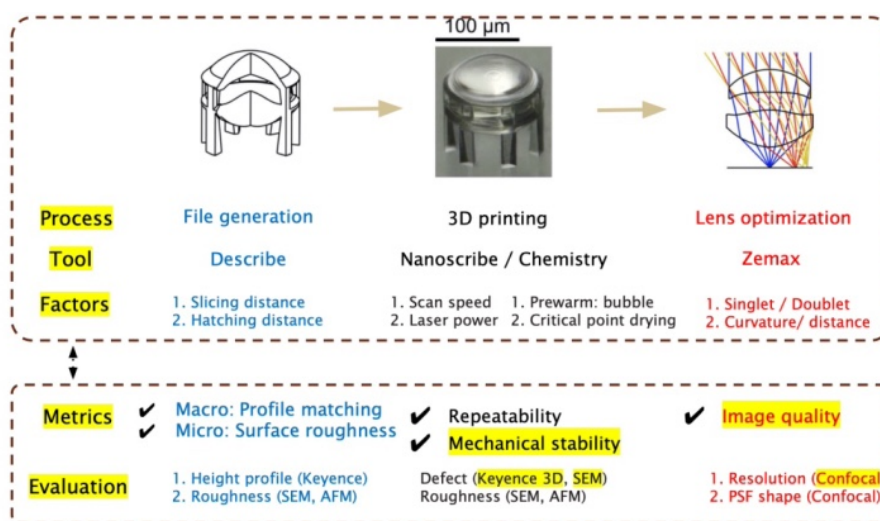

Figure 1: Process flow and optimization metrics for the microlens experiments. Each process includes corresponding metrics and evaluation methods.

The STL files could be generated from 3-D CAD software(AutoCAD, Solidworks, Tinker-CAD, Blender, etc.). We chose Zemax OpticStudio for STL file generation because of its powerful and convenient ray tracing and image simulation capabilities. After generating designs with desired curvatures, we added structural supports and outputted the STL files. Describe was used to convert STL files to writing sequences. In Describe, we generated job files and defined parameters, including hatching distance and slicing distance for the writing. The writing laser power and scan speed were defined in the GWL file for the printing. These parameters highly affect writing accuracy and performance.

At the two-photon polymerization stage, the Nanoscribe GT system was used to perform the writing. ITO-coated glasses (25 mm x 25 mm x 0.7 mm, ITO film $\simeq$ 18 nm) were used as the substrate. IP-S negative tone resin (refractive index = 1.478 @ 20C, Nanoscribe)[4] was drop-casted on the conductive side of the substrate for printing. Before printing, the substrate with resin was preheated under 60 degrees on a hotplate. The preheat helps avoid the bubbles in the resin and significantly enhances the printing reproducibility. To perform dip-in laser lithography (DiLL), we loaded the substrate with a DiLL holder and flipped it upside down for insertion. A 25x objective (NA=0.8) with adjustment ring set on Glyc and a 780 nm laser were used for the printing. The designed structures are written layer-by-layer with a piezo stage that controls the axial direction, and Galvo mirrors control the lateral direction. After the printing process, the structures are developed with the SU8 developer for thirty minutes and then under isopropanol or HFE-7100 (3M Novec) for ten minutes for washing out the developer.

In micro-optics printing, the surface profile and smoothness matter the most for the optical performance. Therefore, we screened out mainly laser power and scan speed to achieve the best smoothness. The printing results were evaluated in terms of repeatability and mechanical stability with Keyence 3-D microscope and scanning electron microscopy (both 0 and 90 degrees). Keyence Laser confocal microscope provides surface profile. Atomic force microscopy (AFM) and scanning electron microscopy (SEM) reveals the surface roughness information.

To achieve the best functionalities of the microlens, we performed a series of simulation and functionality tests to suggest further optimization. For this purpose, we performed the simulation experiments with Zemax OpticStudio and evaluated the functionalities with imaging and point spread function (PSF) measurements.

2.2 Factors affect microoptics printing

We want to highlight factors especially crucial in the micro-optics printing process:

Slicing distance is the most critical printing parameter because too large slicing distance is the main reason to cause staircase effect (Figure 2). Therefore, we highly recommend setting the slicing distance equal to 100 or 200 nm for micro-optic applications. The hatching distance is relatively less important and could be set to 200 nm to save the printing time.
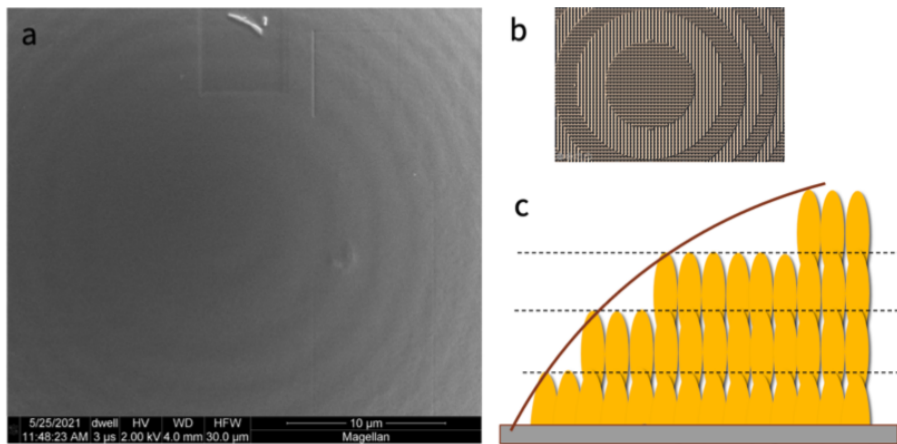

Figure 2: Staircase effect results from the slicing. 2a. SEM image to reveal staircase effect. 2b. A Describe display that defines the staircase when slicing. 2c. Illustration of staircase effect.

2.3 Job file preparation

We start with STL files output from CAD software and demonstrate the writing sequence generation steps by steps (Figure 3).
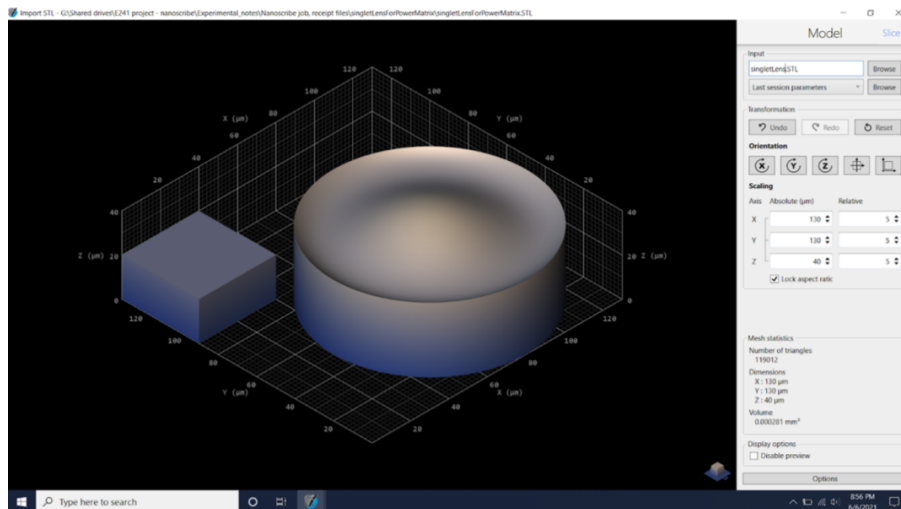

Figure 3: An example of Describe display after importing a STL file

When we import our STL structures, we could see a display like this. In this display, scaling factors are specified to define the structures on the correct scale. The Describe uses a default unit in micron for STL files, which might cause some design issues. One can visualize one common issue in this step by a very rough structure at this step. This issue suggests that the STL does not include enough mesh points. If this issue occurs, consider drawing the structures larger or define the structures with more mesh points to solve the problem. Another helpful information is volume under the mesh statics, and this value can be used to estimate the rough printing time. In the parameter sets provided in this document(25x objective, IP-S resin, hatching 200 nm, slicing 100 nm), the printing time is roughly 0.013 mm^3/hr. Another valuable tip is to restrict the writing block size within 300 x 300 x 300 um size when using 25x objective. The writing accuracy slightly deteriorates when writing is close to the block border. Put structures in the center of the writing field if possible. Also, if the structures are larger than 300 um and this would involve multiple writing blocks for the writing. Since stitching between writing fields involves some artifacts, one should beware of avoiding the stitching happening in the functionality part of the design.

We chose the solid mode for our printing to achieve the best structural integrity and homogeneity. We set the slicing distance as 100 nm or 200 nm and the hatching distance as 200 nm for the best prototyping of the printing. The hatching angle is the angle between two consecutive layers for the writing direction. This angle is 90 degrees to minimize a directional artifact inside the structures and retain the shape accuracy. Our structures adopt a constant exposure, but the shell-and-scaffold printing method can also be investigated. For other parameters, one can use the settings below as a starting point (Figure 4). NanoGuide provided by the Nanoscribe company also has a clear explanation for each parameter setting.

After deciding all the parameters for the writing sequence, we will see a GWL file with parameters for the control system. Laser power and scan speed are the most important power to be changed in this window. Next, click Generate 3D Preview under the 3D Preview drop-down menu to estimate the writing time (Figure 5).

After defining the parameter sweep, one should see the window as below, and it means the parameter sweep file has been successfully created (Figure 6).
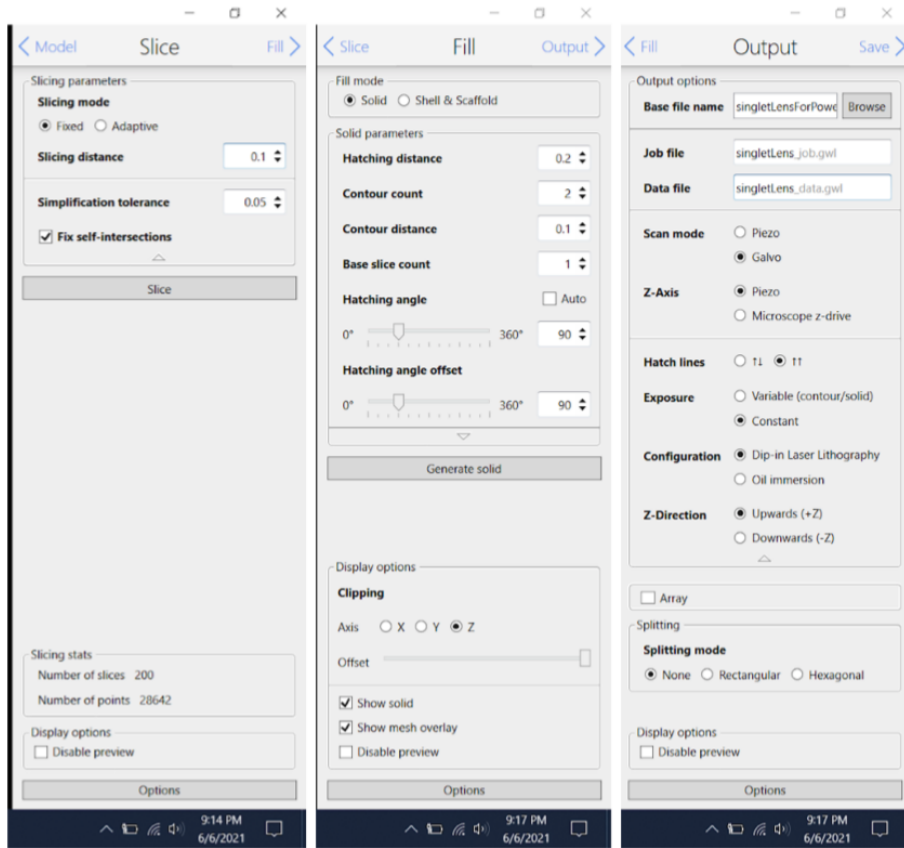
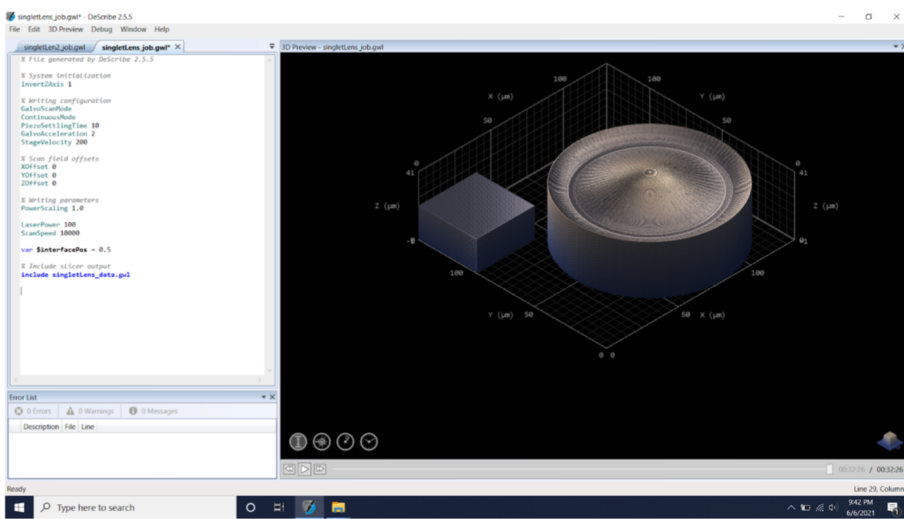Figure 4: An example of parameter setting in Describe

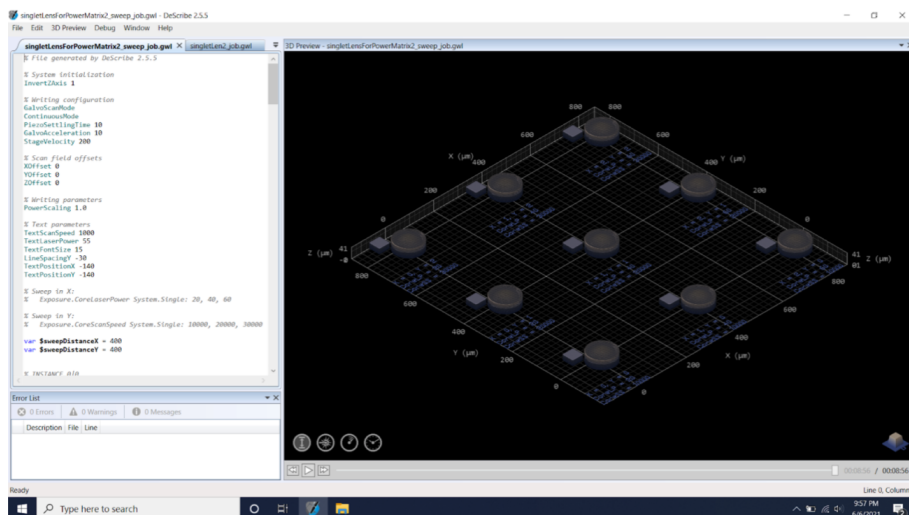Figure 5: An example of GWL code for defining laser power and scan speed

Figure 6: A final display after the advanced STL processing

2.4 Development

For the development, the standard processing is 30 minutes SU8 developer followed by 10 minutes IPA. Depending on the structural complexity, users could decide the SU8 developer development time to achieve the best efficiency. However, in IPA drying, the tension created by the solvent could potentially collapse the delicate structures. Therefore, several development methods are implemented to deal with this issue and minimize structural deformation during drying.

The first way is using HFE-7100 for drying. HFE (or hydrofluroether) consists of a complex cleaning solvent that does not occur naturally in the environment. The advantage of HFE solvent is having a very low surface tension and could preserve structural integrity.

The second way is using a critical point dryer to remove the IPA. It eliminates surface tension associated with liquid drying by avoiding the phase transition boundary from liquid to gas. Here we show an example using HFE as a rinse solvent to preserve an overhanging structure for microlens.

2.5 Characterization procedure

We establish a series of characterization procedures to evaluate our micro-optics fabrication in the hope of answering a different question based on our designed metrics. This study uses SEM, AFM, laser confocal microscope, and 3D microscope as our main characterization tools. This characterization logic is generalizable for other two-photon polymerization processes.

SEM provides a way to evaluate the surface property and internal structure of the lens. This technique can provide qualitative information of surface property after printing. For example, SEM reveals the staircase effect after printing and helps us evaluate the smoothness of the structures for the following images. We also figure out a 90-degree SEM procedure for the evaluation of the internal structures. The 90-degree SEM is helpful if some residues or deformations exist in the internal structures.

For other tools, AFM can reveal microscopic surface smoothness properties. Keyence laser confocal microscope provides topography and height information, allowing us to match surface profile. Keyence 3D microscope visualizes the lens in multiple angles from 0 degrees (top images) and 90 degrees (side image). Also, Keyence 3D can be operated in a transmissive or reflective mode to provide different contrast.

3 Results

3.1 Writing condition optimizations

To optimize the microlens quality, we performed the parameters sweep of laser power and scan speed to see how exposure affects surface roughness. The figure below illustrates the transmission image of the microlens under different laser power and scan speed. We increase the laser power from 20%, 40%, 60%, and scan speed from 20000, 40000, 60000 um/s, respectively. As shown in the red dotted box, we showed that microlens has better surface smoothness under the higher laser power and the lower scan speed condition. This better smoothness is the result of the proximity effect of adjacent polymerization of IP-S resin. The stronger the laser power, the larger the voxel of the lasers point spread function above the polymerization threshold. This larger voxel size causes more overlap between the adjacent single voxel and better smoothness.
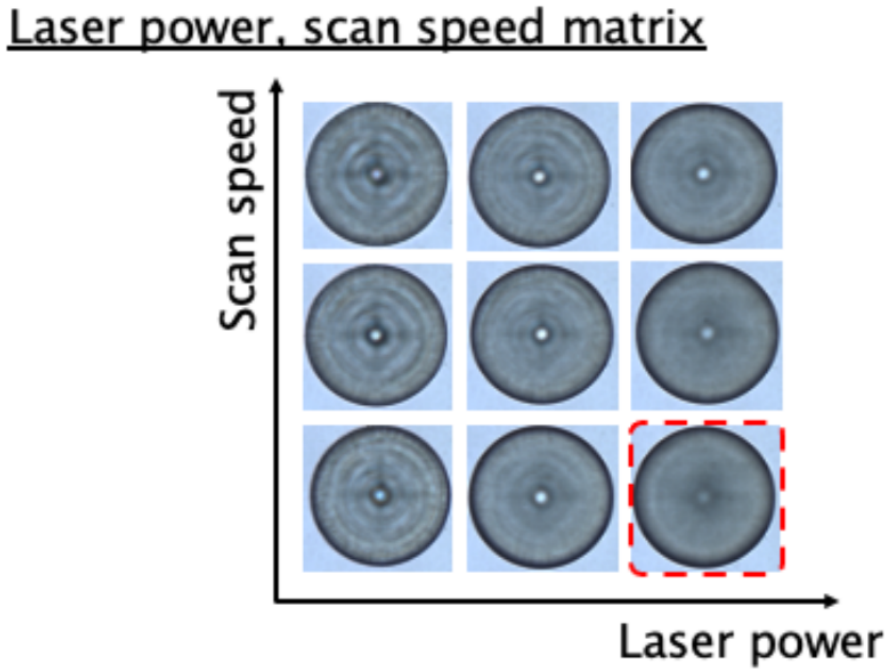

Figure 7: Optical images of microlenses reveal different qualities of surface roughness under different exposure conditions.

3.2 Characterizations

3.2.1 Optical imaging

The advantages of optical imaging is its accessibility and ability to view in different contrast. Multiple contrast including transmission, reflection, side view and dark field image. Different choices of contrast allows us to identify different writing defects.

Side view imaging Side view images from keyence 3D microscope provide direct structural information. As we rotate the sample by 90 degrees, the microscope can directly visualize the lens from the side. As we tape our sample on a pre-tilt stand in 90 degrees, the microscope can directly visualize the lens from the side for the visualization of hollow structures (Figure 8a, b). The blurry image in the back is the second row of the sample with different height. The actual size and the design structure is shown in the right image (Figure 8c).
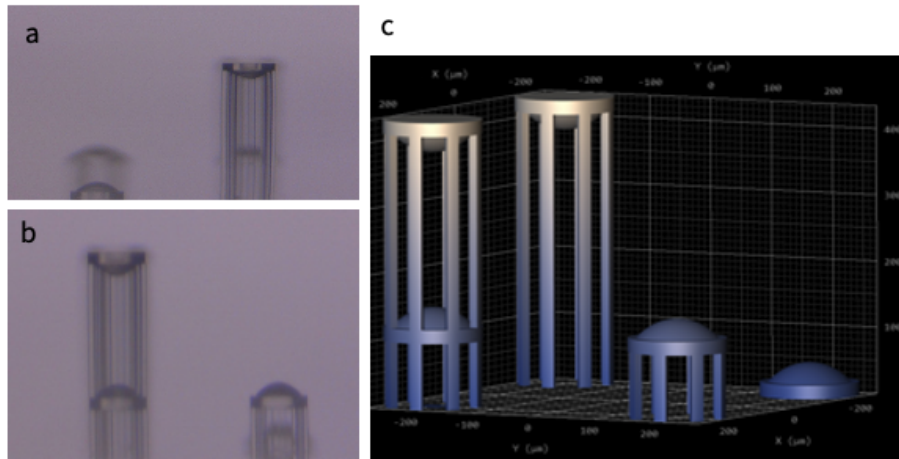
Figure 8: High-aspect ratio overhanging structures. 8a, b. Keyence 3D imaging on 90 pre-tilt substrates. 8c. STL Design of the printed structures.

Transmission, reflection and dark field imaging Transmission images highlight any absorption and scattering contrast inside the lens structure, while reflection images mainly reflect the backscattering in the air polymer interface. The below images show the transmission (Figure 9a), reflection (Figure 9b), and dark field (Figure 9c, d) image of the microlens and the flat substrate under 60% laser power and 20000 um/s scan speed with a slicing distance of 100 nm. Both the transmission and reflection image shows a grid-like pattern related to the laser scanning trajectory. The transmission image provides more valuable information about the microlens. The reflection image only highlights the center of the top surface. On the other hand, the reflection images highlight some additional structural features such as surface roughness and defects. In the dark field image, the scattering of surface roughness and the staircase from the top surface is dominant.
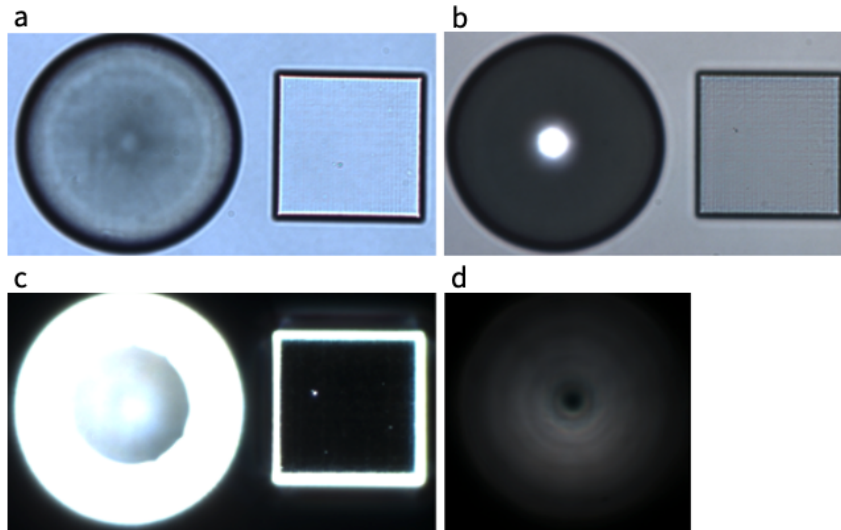

Figure 9: Transmission, reflection, and dark field imaging for simple microlens. 9a. Transmission image provides more structural information for the microlens. 9b. The reflection image highlights the center of the top surface. 9c. Darkfield imaging reveals the scattering of surface roughness and the staircase from the top surface. 9d. A dark field image with a shorter exposure time.

Confocal imaging   The images coming from a wide field detector cannot give high resolution and provide the optical section. Instead, confocal imaging provides an optical section that allows us to characterize the doublet lens's hollow structure better. For example, the confocal images show three Z stacks inside the microlens: 0, 20, 40 microns in transmission contrast (Figure 10). Thus, we can observe and distinguish the rod and lens structure apart.
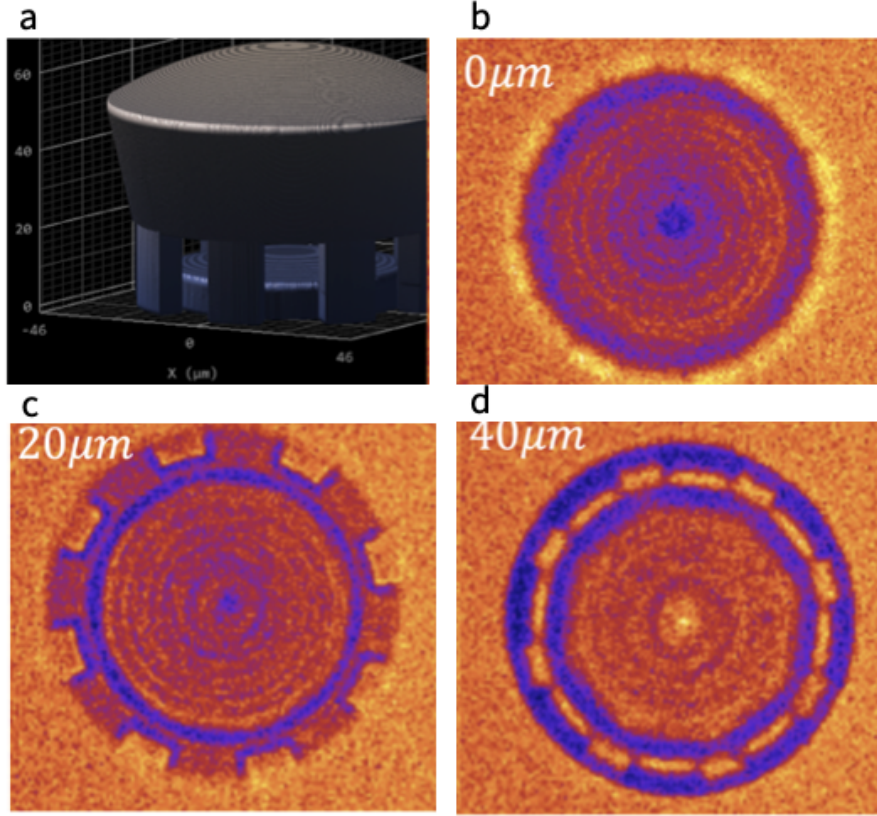

Figure 10: Confocal imaging provides information along the z-axis for doublet. 10a. STL design of doublet. 10b. Confocal image at the top of the structure. 10c. Confocal image in the middle of the structure. 10d. Confocal image at the bottom of the structure.

Scanning Electron Microscopy (SEM)   SEM is a valuable technique to provide qualitative information for the printed structures. Our structures have overhanging structures, and it is not possible to get inner structure information from a top-down image. Therefore, we developed two 90-degree SEM strategies for this inner structure evaluation. The images were taken by taping substrate on a 45-degree pre-tilt stub and tilt another 45 degrees to get a 90-degree angle for the imaging. The substrate has a relatively long working distance compared to the standard SEM imaging to prevent the substrate from hitting the metal pole. One worth-mentioning observation is that the substrate would block some parts of the electron for the imaging, so the images have shallow contrast. The 90-degree SEM could be taken on a full-printed structure (Figure 11a). We noticed that a mystery string appears inside of the inner structure if the lens was printed at the origin. The 90-degree SEM can also be taken on a half printing structure(Figure 11b), and in this way, the inner curvature profile could be visualized.

Keyence confocal profile   Keyence confocal microscope provides topography and height information, and this allows us to match surface profile. We plot the actual design of microlens and the actual topology acquired by the Keyence confocal microscope. Keyence laser scan in 3D on the top surface of the lens and provide good spatial resolution. The overlay curve between actual printing and Zemax design shows the high accuracy of the printing result. (Figure 12)
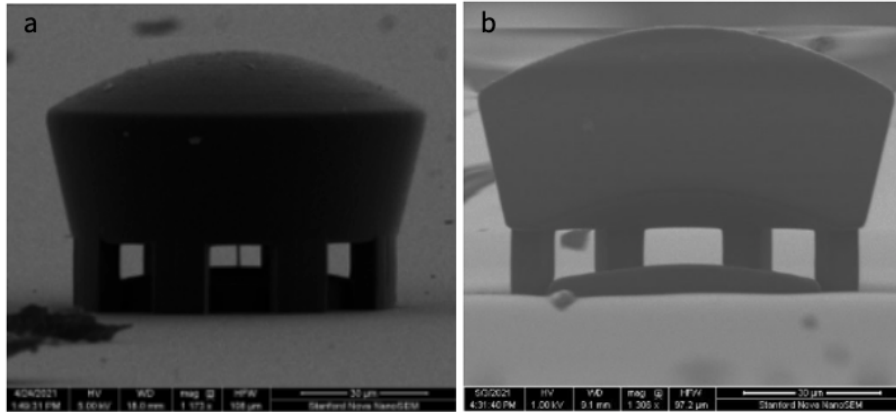
Figure 11: 90-degree SEM images for characterizing inner structures of doublets.11a. Vertical SEM helps identify a mystery string inside of an overhanging structure. 11b. Characterization on a half printing structure allows the visualization of inner lens curvatures.
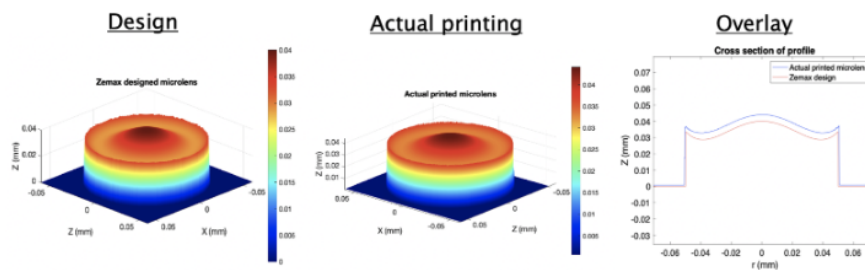

Figure 12: A laser confocal microscope measurement reveals the profile of the printed microlenses. 12a. Design profile generated from Zemax. 12b. The 3D profile was measured by Keyence laser confocal microscope. 12c. The overlay surface profile between the design and the printed structure.

3.2.2 Functionality tests

In our experiments, we fabricated finite and infinite conjugate lenses. We performed several optical characterizations to demonstrate the functionalities of the printed lens. For finite-conjugate lenses, we obtained imaging and evaluated the imaging quality from the printed microlens with an optical setup. We also designed an infinitely conjugated lens for better functionality in future endoscope design.

Infinite conjugate lens functionalities For an infinite conjugate lens, a collimated beam can be focused to a single point by an infinite conjugate lens. The characterization of the focus represents several valuable parameters such as the spatial resolution, the point spread function (PSF) shape, and the focal length.

The setup to create the collimated beam and characterize the resulting focus is shown in Fig. 13 left panel:

(1) An acousto-optic tunable filter (AOTF) was used to select 588 nm wavelengths from a supercontinuum laser source.

(2) The laser was fiber-coupled and collimated by a fiber collimator into free space. The collimated laser beam was then focused by microlens to form a tight focus.

(3) The focus was imaged using a high numerical aperture (100x, NA = 0.9) objective into a microscope system (Nikon Eclipse upright) for either confocal scanning images or wide-field CCD images.

After determining the focus in the focal plane, the working distance can be calculated by subtracting the focal plane of Z with the top of the lens. The experimental working distance of 108um matches the design.

By further analyzing the PSF, we calculated the spatial resolution and the focus shape. The spatial resolution was determined by the full width at half maximum (FWHM) length at the focus. The resulting FWHM is 0.7 um, which matches with the designed 0.69 um. Second, the focus shape was visualized through PSF analysis. The circular shape PSF implies a circularly symmetric printed lens.
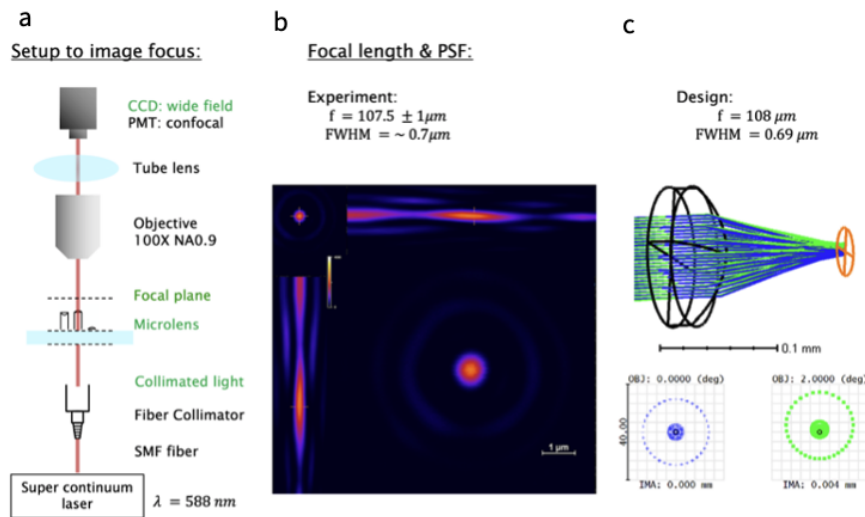

Figure 13: Characterization of the infinite conjugate lens. 13a. The setup for characterization of PSF for an infinite conjugate lens. 13b. PSF shape measured from the setup. 13c. Simulation of PSF matches the experimental data.

Finite conjugate lens functionalities For finite conjugate singlet and doublet lens, we demonstrated the image quality of our printed lens qualitatively. First, a tissue sample was used as our test object for imaging and illuminated by a halogen light source and a condenser. Next, the printed microlens project an image of this tissue sample in the image plane. The resulting

image is consequently imaged using a 20x NA 0.45 objective to the microscope system. Fig 14 shows different images of the tissue sample using our printed singlet and doublet with different magnification.
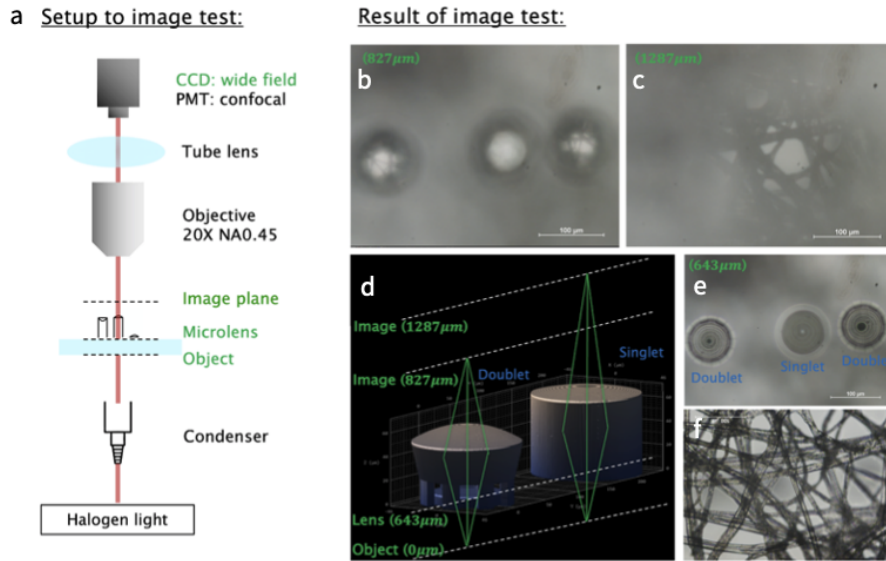

Figure 14: Characterization of images acquired by the finite conjugate microlens. 14a. The setup for image characterization for a finite conjugate lens. 14b. A resulting image from a doublet (center) at 827 um from the object. 14c. Lens design and focal planes illustration. 14d. A resulting image from a singlet at 1287 um from the object. 14e. The microlens structure could be visualized at 643 um from the object. 14f. The actual object image.

4 Conclusions

In this report, we demonstrated the fabrication of infinite and finite micro-lenses. We introduced tips and tricks in every aspect of two-photon polymerization, including file preparation, parameter choosing, pre-processing, development, and post-processing. In addition, we establish a helpful characterization process flow and exemplify the logic to troubleshoot the process. Our engineered structures gave rise to successful optical measurements, and the results were matched with the simulation. Our process flow can benefit people in the nanofabrication and photonics community. In the long term, we hope to integrate our printed micro-lensed into the endoscope and provides a better tool for neuroscience.

5 Future works

In the future, we will establish a miniaturized 4f cage system. The four-step procedure is outlined below. First, we will start with a simulation of a single lens for a designed working distance of 100 microns. The effective focal length will be used in the next step. In step two, we will combine two singlet lenses into a 4f cage system. Next, the STL file will be generated for inspecting each step of the printing process. Finally, the structure will be printed and proceed with further characterization.

References

[1] A. Antonini, et al. Extended field-of-view ultrathin microendoscopes for high-resolution two-photon imaging with minimal invasiveness. *eLife*, 9:e58882, 2020.

[2] T. Gissibl, et al. Sub-micrometre accurate free-form optics by three-dimensional printing on single-mode fibres. *Nature Communications*, 7:11763, 2016.

[3] T. Gissibl, et al. Two-photon direct laser writing of ultracompact multi-lens objectives. *Nature Photonics*, 10:554–561, 2016.

[4] T. Gissibl, et al. Refractive index measurements of photo-resists for three-dimensional direct laser writing. *Opt. Mat. Exp.*, 7:7, 2017.

[5] H. Pahlevaninezhad, et al. Nano-optic endoscope for high-resolution optical coherence tomography in vivo. *Nature Photonics*, 12:540–547, 2018.

[6] M. A. Tadayon, et al. Microphotonic needle for minimally invasive endoscopic imaging with sub-cellular resolution. *Scientific Reports*, 8:10756, 2018.

[7] S. Thiele, et al. 3d-printed eagle eye: Compound microlens system for foveated imaging. *Science Advances*, 3:e1602655, 2017.

[8] W. Yuan, et al. Fabrication of microlens array and its application: A review. *Chin. J. Mech. Eng.*, 31:16, 2018.